A preliminary assessment of the failed and successful predictions of proton spectral hardness using microwave emission

WP2 Team (OBSPARIS, NOA, UMA) Leader:Marlon Nunez

August 26, 2016

1 Purpose

Task 2-2 of the HESPERIA project aims at investigating if the hardness or softness of the proton spectrum in interplanetary space can be predicted from the shape of the microwave spectrum. The technique developed by Chertok et al (2009) is to use the ratio of peak microwave flux densities near 9 and 15 GHz as a predictor: hard proton spectra (characterized in Chertok et al (2009) and in the following by the logarithm of the ratio of the proton intensities above 10 MeV and above 100 MeV,

$$\delta = \log \frac{J(E > 10 \text{ MeV})}{J(E > 100 \text{ MeV})}$$

are predicted when the high-frequency microwave emission is important - that is, when the ratio of the 9 GHz flux density to the 15 GHz flux density is low, whereas steep proton spectra are predicted when this ratio is high. The purpose of the present document is to re-evaluate this tool, and to discuss when it works, when not, and why it fails in certain cases. We also assess if the flux density ratio used by Chertok et al (2009) can be replaced by another parameter, namely the peak frequency of the microwave spectrum.

2 Gyrosynchrotron spectrum

Gyrosynchrotron emission from non thermal electrons in the energy range between several tens of keV and a few MeV produces a characteristic special shape: the flux density rises with increasing frequency in the GHz range to a spectral peak that, depending on the event, lies between a few GHz and a few tens of GHz, and then decays with increasing frequency beyond the peak. A typical spectrum as observed by the RSTN solar radio telescope network is shown in Figure 1. The spectrum is optically thick below the peak frequency, and optically thin above. The spectral index in the optically thin part is directly related

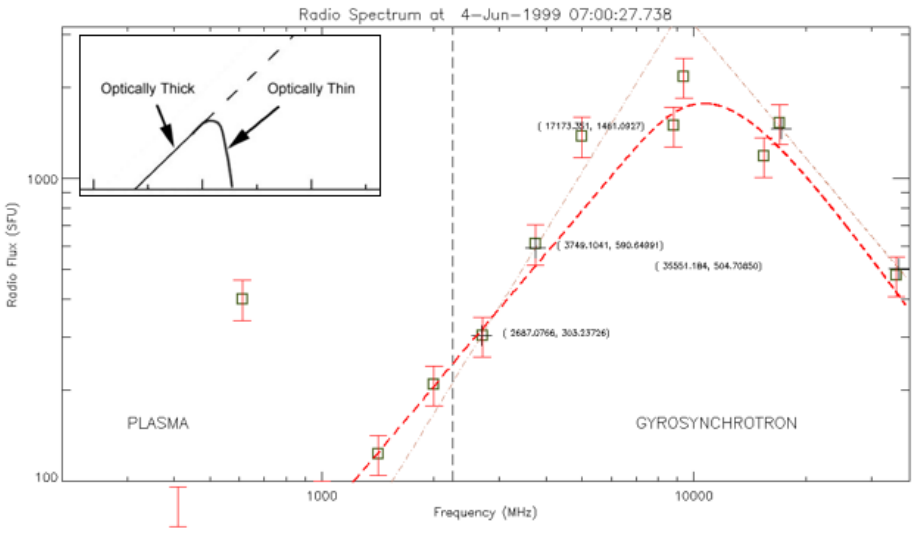

Figure 1: A typical microwave burst spectrum as produced by gyrosynchrotron emission (HESPERIA). The inset indicates the part of the spectrum in the optically thin or optically thick regime.

to the index of the energy spectrum of the radiating electrons. The prediction of a hard SEP spectrum is hence based on an observed hard spectrum of the microwave emitting electrons when the spectrum is optically thick with a peak frequency below 9 GHz, so that both 9 GHz and 15 GHz are located in the optically thick part of the spectrum.

Chertok et al (2009) use the ratio of peak flux densities near 9 and 15 GHz. If both frequencies are in the optically thin part of the gyro synchrotron spectrum, this ratio is always greater than unity. The electron spectrum is the harder, the closer the ratio is to 1. The result is not directly related to the electron spectrum when the two frequencies are on different sides of the peak frequency, or when they are both on the optically thick side. In the latter case the ratio of flux densities is always smaller than 1. Chertok et al (2009) find a correlation with broad scatter between S_9/S_{15} (values varying between about 0.4 and 2.7) and the steepness of the proton spectrum (δ, values varying between about 0.3 and 2.8). Their figure 1 shows especially that when $S_9/S_{15} < 1$, $\delta < 2.5$: harder proton spectra in space are associated with microwave bursts whose peak flux density is higher near 15 GHz than near 9 GHz. This means that harder proton spectra tend to occur when the microwave emission is optically thick up to the highest observing frequency of RSTN, 15.4 GHz. If employed as in Chertok et al (2009) the flux density ratio has nothing to do with the high-frequency spectral index, that is, with the flatness or steepness of the energy

spectrum of the microwave-emitting electrons. It is rather related to the number of the non thermal electrons, but also to the magnetic field intensity in the source. We are therefore addressing an empirical relationship rather than a well-defined physical relationship.

In the following we re-evaluate the relationship between the microwave spectrum at the Sun and the proton spectrum at 1 AU using SEP events between 1997 and 2006. The ratios of the peak microwave flux densities and the spectral indices of the protons are displayed in Table 1. We use the convention that the S_9/S_{15} ratio predicts a "hard" proton spectrum when < 1, and a soft one when > 1. We call the observed proton spectrum "hard" when $\delta < 1.5$, and "soft" when $\delta > 1.5$. A successful prediction is when the predicted and observed qualification of the proton spectrum are the same. The predicted hardness of the proton spectrum and the observed one are listed in col. 4 of Table 1. Column 8 gives the quality of the prediction: A and D are successful predictions of either a hard or a soft proton spectrum. B is an erroneous prediction (hard spectrum predicted, but soft spectrum observed), as well as C (soft spectrum predicted, but hard spectrum observed). Column 9 gives the category of the event.

3 Analysis of the events

3.1 SEP analysis

We selected a list of events for the period from November 1997 to May 2013 using the online GOES > 10 MeV proton list available at SPWC (http://umbra.nascom.nasa./gov/SEP/) together with a SEP event list provided at >100 MeV energy compiled with 1 pfu threshold criterion and with the following parameters available: event date, onset time, peak time and peak intensity.

The SEP analysis was carried out collecting data either from GOES-8, GOES-9 or GOES-10 by selecting the reference spacecraft as recommended by NOAA for each time period. For the purposes of the prototype tool (Deliverable D2.3) the period 1997-2006 was selected for initial study and the number of events was increased with respect to the Year 1 Report of HESPERIA. During this period intervals of large and low solar activity occurred, in which a large number of >10 and > 100 MeV SEP events took place, whose solar associations have been extensively studied. Inspection of the SEP events reported in the GOES list showed that there were cases of SEP events which had reported enhancement at 10 MeV, cases which had reported intensity enhancements both at 10 and 100 MeV, and cases with only peak intensities at 100 MeV reported. After inspection of the GOES plots it was recognised that the last category of SEP events occurs shortly in time (of the order of 1-2 days) after a strong SEP event with intensity of several 100s pfu. Thus, the proton intensity level at 10 MeV was elevated during this time period (above 10 pfu) and it did not qualify as a new SEP event according to the NOAA criteria. For this reason there was no newly reported SEP injection at 10 MeV but only at 100 MeV where the pre-event background was low. Such cases have been excluded from the analysis. Sufficient data

	Date Flare	Date SEP	Location	S_9/S_{15} / δ	Peak frequency [GHz]	SEP spectrum predicted	SEP spectrum observed	Quality of Prediction	Category
1	1997 Nov 06 11:55	Nov 06 12:50	S18 W63	0.47 / 0.45	15.4	hard	hard	A	Multi Peak
2	1998 May 02 13:42	May 02 14:00	S15 W15	2.34 / 1.3	8.8	soft	hard	C	Multi Peak
3	1998 May 06 08:09	May 06 08:25	S11 W65	1.51 / 1.85	8.8	soft	soft	D	Multi Peak
4	1998 Aug 24 22:12	Aug 24 23:10	N30 E07	2.16 / 1.70	4.9	soft	soft	D	Single Peak
5	1999 Jun 04 07:03	Jun 04 08:50	N17 W69	1.26 / 2.44	10	soft	soft	D	Single Peak
6	2000 Apr 04 15:41	Apr 04 17:05	N16 W66	1.46 / 2.76	2.9	soft	soft	D	Single Peak
7	2000 Jul 22 11:34	Jul 22 12:25	N14 W56	1 / 1.69	8.8	soft	soft	D	Single Peak, Thermal
8	2000 Nov 08 23:28	Nov 08 23:35	N05 W77	1.87 / 1.49	8.8	soft	hard	C	Single Peak
9	2000 Nov 24 05:02	Nov 24 07:20	N20 W05	0.36 / 1.38	17	hard	hard	A	Single Peak
10	2000 Nov 24 15:13	Nov 24 16:30	N22 W07	0.54 / 1.88	15.4	hard	soft	B	Multi Peak
11	2001 Mar 29 10:15	Mar 29 13:00	N24 W12	1.53 / 2.16	8.8	soft	soft	D	Single Peak
12	2001 Apr 02 21:51	Apr 02 23:15	N14 W82	0.47 / 1.45	15.4	hard	hard	A	Multi Peak
13	2001 Apr 10 05:26	Apr 10 08:30	S23 W09	1.39 / 2.38	8.8	soft	soft	D	Multi Peak
14	2001 Apr 15 13:50	Apr 15 14:10	S20 W85	0.28 / 0.81	15.4	hard	hard	A	Multi Peak
15	2001 Apr 26 13:12	Apr 27 00:55	N17 W31	1.50 / 2.02	8.8	soft	soft	D	Single Peak
16	2001 Sep 15 11:28	Sep 15 12:50	S21 W49	1.26 / 1.82	4.9	soft	soft	D	Confined
17	2001 Oct 19 16:30	Oct 19/1840	N15 W29	1.59 / 1.58	8.8	soft	soft	D	First Peak Confined
18	2001 Oct 22 17:59	Oct 22/1815	S18 E16	0.64 / 1.44	15.4	hard	hard	A	Confined
19	2001 Nov 04 16:20	Nov 04/1640	N06 W18	1.79 / 1.32	8.8	soft	hard	C	Single Peak
20	2001 Nov 22 23:30	Nov 23 00:15	S15 W34	2.90 / 3.07	4.9	soft	soft	D	Single Peak
21	2001 Dec 26 05:40	Dec 26 05:50	N08 W54	2.14 / 1.19	8.8	soft	hard	C	Single Peak, Shock
22	2002 Feb 20 06:12	Feb 20 07:00	N12 W72	1.29 / 2.72	9.4	soft	soft	D	Single Peak
23	2002 Apr 17 08:24	Apr 17 11:35	S14 W34	2.63 / 3.08	4.9	soft	soft	D	Multi Peak
24	2002 Apr 21 01:51	Apr 21 02:00	S14 W84	2.06 / 2.04	8.8	soft	soft	D	Multi Peak
25	2002 May 22 03:54	May 22 08:05	S19 W56	1 / 2.31	8.8	soft	soft	D	Single Peak, Thermal
26	2002 Jul 15 20:08	Jul 16 13:40	N19 W01	1.35 / 3.11	8.8	soft	soft	D	Multi Peak
27	2002 Aug 14 02:12	Aug 14 03:55	N09 W54	3.90 / 3.11	2.9	soft	soft	D	Low flux density
28	2002 Aug 22 01:57	Aug 22 03:05	S07 W62	1.78 / 1.32	4.9	soft	hard	C	Single Peak, Confined
29	2002 Nov 09 13:23	Nov 09 16:10	S12 W29	1.54 / 3.68	4.9	soft	soft	D	Single Peak
30	2003 May 28 00:27	May 28 07:25	S07 W17	1.60 / 1.76	8.8	soft	soft	D	Multi Peak
31	2003 May 31 02:24	May 31 03:00	S07 W65	0.73 / 1.49	15.4	hard	hard	A	Multi Peak
32	2003 Oct 26 18:19	Oct 26 18:05	N02 W38	1.35 / 2.64	8.8	soft	soft	D	Multi Peak
33	2003 Oct 28 11:10	Oct 28 12:15	S16 E08	1.17 / 1.52	8.8	soft	soft	D	Saturated
34	2003 Nov 20 23:53	Nov 21 06:05	N02 W17	2.42 / 2.3	3.9	soft	soft	D	Multi Peak
35	2004 Apr 11 04:19	Apr 11 06:10	S14 W47	2.18 / 2.35	5.4	soft	soft	D	Single Peak
36	2004 Sep 12 00:56	Sep 13 20:00	N04 E42	2.19 / 3.22	3.4	soft	soft	D	Multi Peak
37	2004 Nov 07 16:06	Nov 07 18:25	N09 W17	1.77 / 2.96	5.4	soft	soft	D	Multi Peak
38	2005 Jan 17 09:52	Jan 17 13:05	N15 W25	1.19 / 2.25	5.4	soft	soft	D	Multi Peak
39	2005 Jan 20 07:01	Jan 20 06:55	N12 W58	0.7 / 0.46	35	hard	hard	A	Single Peak
40	2005 Jun 16 20:22	Jun 16 20:50	N09 W87	2.7 / 1.17	5.4	soft	hard	C	Single Peak, Low flux density, Strong Type II
41	2005 Jul 14 10:34	Jul 14 13:40	N10 W80	0.90 / 2.81	15.4	hard	soft	B	Multi Peak
42	2005 Jul 27 05:02	Jul 27 23:00	N11 E90	1.65 / 2.31	5.4	soft	soft	D	Multi Peak
43	2005 Aug 22 17:27	Aug 22 19:30	S12 W60	1.16 / 2.95	8.8	soft	soft	D	Multi Peak
44	2005 Sep 07 17:40	Sep 07 21:50	S06 E89	0.61 / 1.09	15.4	hard	hard	A	Multi Peak
45	2006 Dec 06 08:23	Dec 06 15:10	S04 E63	2.75 / 3.79	8.8	soft	soft	D	Multi Peak
46	2006 Dec 13 02:40	Dec 13 03:10	S05 W23	0.64 / 0.9	22	hard	hard	A	Multi Peak
47	2006 Dec 14 22:15	Dec 14 22:55	S06 W46	1.3 / 1.96	8.8	soft	soft	D	Multi Peak

Table 1: List of SEP events used to predict the spectral hardness using the ratio of flux densities near 9 and 15 GHz.

quality and observing coverage of microwave observations was found for 47 SEP events, allowing the analysis of the microwave flux densities and the calculation of the flux ratio. Figure 2 shows an example of an SEP event analysed in this study. The top panel of the Figure presents 5-min averaged fluxes of the >10 MeV and >100 MeV proton fluxes as measured by the GOES-8 integral channels for the time period 25-29 December, 2001. The bottom panel presents the soft X-ray flux in the 0.1-0.8 nm (1-8 Angström) wavelength range as recorded by the X-ray instrument onboard GOES, with the scales of the flare intensity labeled at the y-axis on the right side of this panel. An intense SEP event is observed on 26 December, in clear association with a M7.0 flare, with maximum observed at 05:40 UT on this day, which occurred at N08W54, i.e. at the western hemisphere of the Sun as viewed from the Earth. The onset of this proton event is relatively fast and exhibits impulsive characteristics, as expected for a well-connected SEP event to the Earth. In most of the SEP events under study it was evident that an incorrect onset time was reported in the SWPC list, due to the 10 pfu intensity threshold criterion used for the compilation of the list, which shifted the actual onset time of the SEP event to be reported considerably later. In all such cases we carried out a re-evaluation of the onset time of the SEP events, identifying the onset time when the proton intensity reached 3 standard deviations above the pre-event background level. The background interval was chosen by an observer separately for each event and the average value of the proton intensity on this interval is used as the background level. The time of the onset of the >10 MeV proton intensity was re-evaluated for the event on 26 December 2001 and is indicated with a blue dot during the risetime of the proton event in Figure 2.

Subsequently, the peak intensities for >10 MeV and >100 MeV as reported in the SEP GOES catalogues were used. For the SEP events when no enhancement were observed at >100 MeV, the background intensity was identified. In Figure 2, the peak intensities reported and used for the SEP event on 26 December 2001 are indicated by the other two blue dots on the proton time profiles. The peak intensities obviously correspond to the highest intensity values attained before decreasing intensities started to be observed, signalling the start of the decay phase of the SEP event. In order to exclude Energetic Storm Particles (ESPs) i.e. contributions by locally shock-accelerated particles in the GOES list at >10 MeV a detailed examination of the GOES proton profiles was carried out for all the 47 events. For 12 cases, the entries for the peak intensities reported in the GOES catalogue were found to be due to an ESP contribution. The peak proton intensity at >10 MeV was re-identified for these 12 events. Figure 3 and Figure 4 show examples of such events. In both Figures, the blue lines correspond to the time of passage of an Interplanetary shock associated with local particle enhancements, whereas the newly identified peak intensities for these events are clearly indicated by the blue dots following the onset of each event. Using the information on the peak intensities at >10 MeV and >100 MeV, the proton spectral index for all the 47 events was calculated as log10 of the ratio of the peak intensity at 10 MeV to the peak intensity at 100 MeV) (as shown in the first equation of the document).

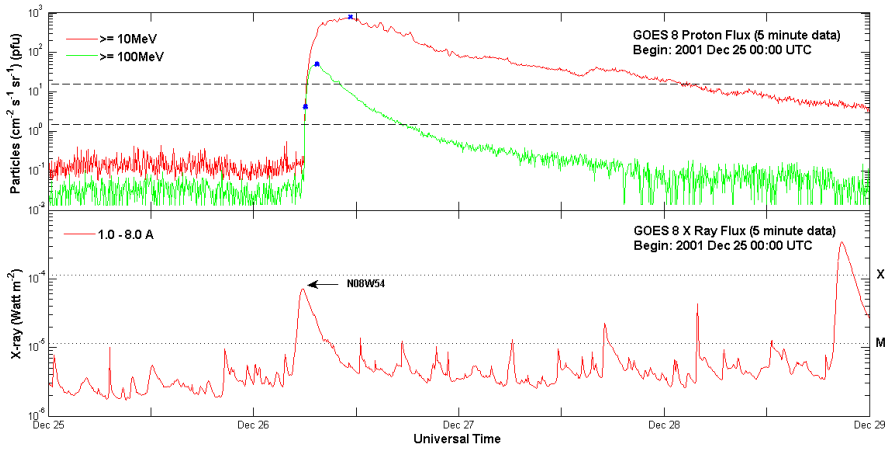

Figure 2: Example of an SEP event observed on 26 December, 2001 associated with an M7.0 flare on this day located at N08W54. The blue dot during the risetime of the event indicates the re-evaluated onset time of the event, whereas the subsequent two blue dots indicate the peak intensities at the >10 MeV and >100 MeV proton channels as reported by GOES.

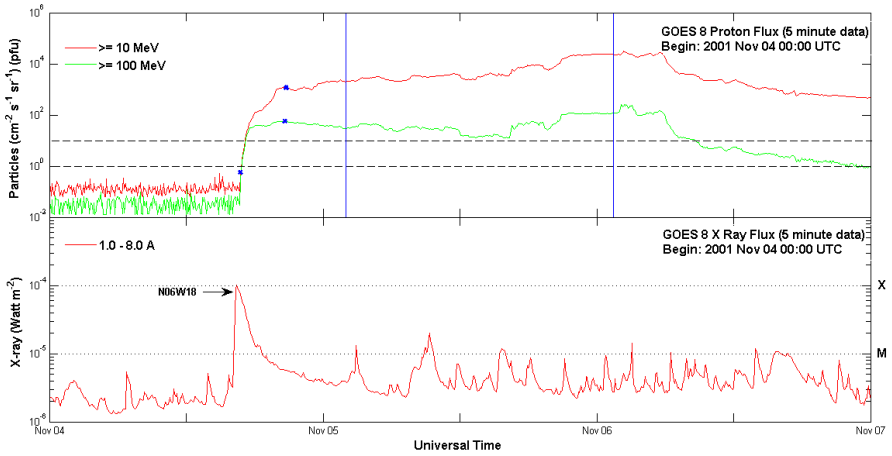

Figure 3: SEP event observed on 4 November 2001, associated with an X1.0 solar flare located at the western hemisphere of the Sun. The blue vertical lines indicate the passage of IP shocks during this period, which evidently have contributions of local shock accelerated particles at both the low and the high energy channels. The newly identified correct peak intensities are indicated by the blue dots following the onset of the event.

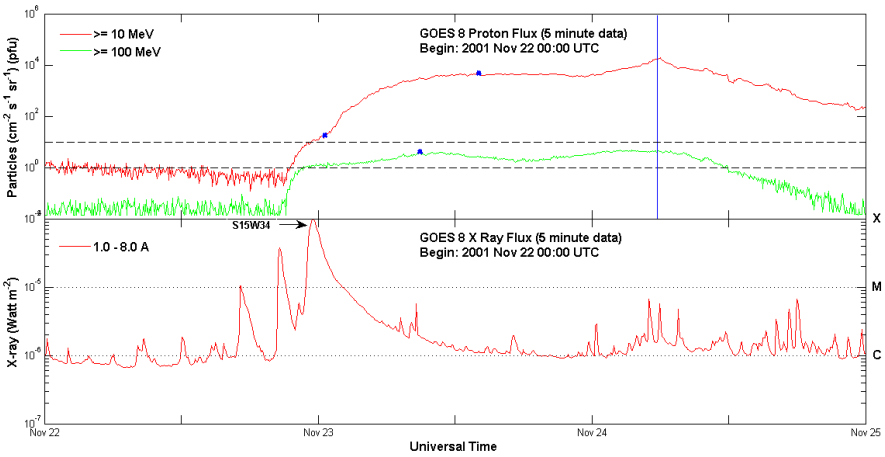

Figure 4: Blue dots following its onset indicate newly identified peak intensities for the SEP event on 23 November 2001 which occurred when the particle intensities were already enhanced due to a previous smaller event. The blue dashed line indicates the time of passage of an IP shock which evidently contributed to local particle increases.

3.2 Discarded Events

Starting from a data-set of 61 events between 1997 and 2006 a sub-set of 47 events where microwave data was available was used for the study. Specifically no microwave data was available for 1997-Nov-04, 1998-Apr-20, 1998-Sep-30, 1998-Nov-14, 2000-Feb-17, 2000-Jun-10, 2000-Jul-14, 2000-Sep-12, 2000-Oct-25, and no microwave burst was recorded for 1998-Nov-14, 2000-Oct-16, 2001-Apr-18. Since these events were reported to occur at the solar limb (W90), an actually existing microwave emission may have been occulted. We therefore discard these events from our analysis. The events on 2002-Mar-15 and 2003-Oct-28 were excluded from the study for instrumental problems, antenna pointing and saturation issues respectively.

3.3 Characteristics of the microwave emission

In order to characterise the different events and understand the potential cause of failed prediction we describe in this section the general properties of the microwave emission and the related solar eruptions. The microwave emission can be divided in two simple categories. One with a simple single peak of the microwave flux density time profile, and another with the presence of multiple peaks where the maximum of the emission at 15.4 GHz and 8.8 GHz may potentially be at different times. The first category allows a simple identification of the peak where the $S_{8.8}/S_{15.4}$ is computed, while the second category

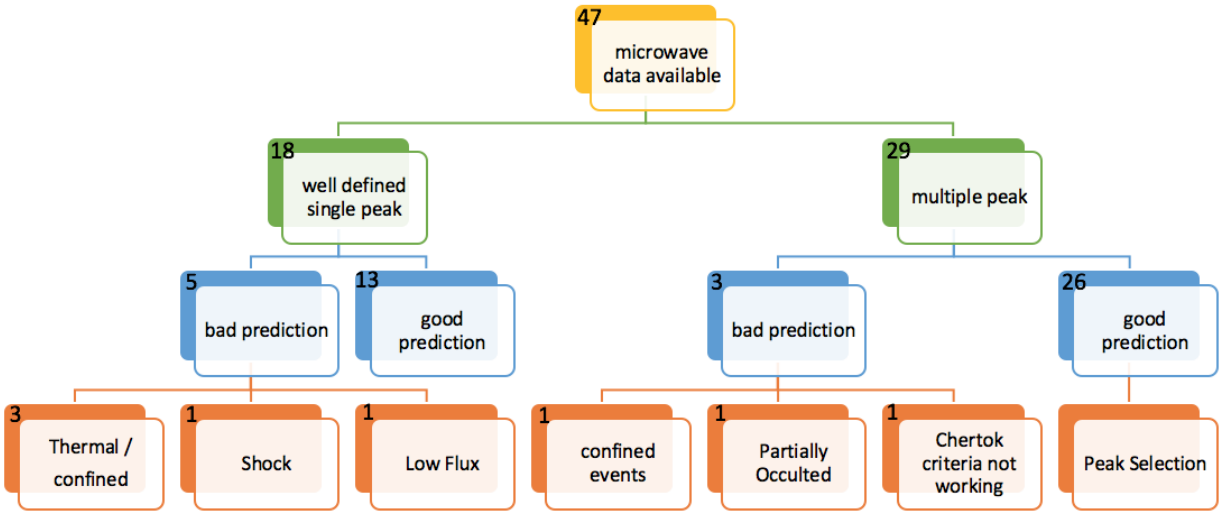

Figure 5: Diagram illustrating the characteristics of the microwave events and the analysis on the false prediction.

requires a more attentive selection of the right peak to take into account to calculate the ratio. A diagram of this classification can be seen in Figure 5. From the 47 starting events 18 showed a well-defined single peak. Specifically events 4, 5, 7, 8, 9, 10, 11, 15, 19, 20, 21, 22, 25, 28, 29, 35, 36 and 40, reported on Table 1 are single peak events. An example plot of a simple single peak event is shown in Figure 6. This category of events returned 5 false predictions. From the remaining 29 events belonging to the multiple peak category, 3 returned a bad SEP spectral prediction. Specifically events 2, 10 and 18 reported on Table 1 returned a false prediction. In the following sections we will describe these events analysing the reason of the spectral prediction failure.

3.4 Thermal Events

The characteristics of the microwave spectrum resulting from accelerating particles at the flare site are due to gyro-synchrotron emission of non-thermal particles. It is possible for certain events where few electrons are accelerated to energies above about 100 keV to observe at microwave frequencies the contribution of thermal particles (bremsstrahlung). This category of events will return a ratio of the microwave emission which is not describing any characteristic of the accelerated particle observed in-situ. An example of this type of

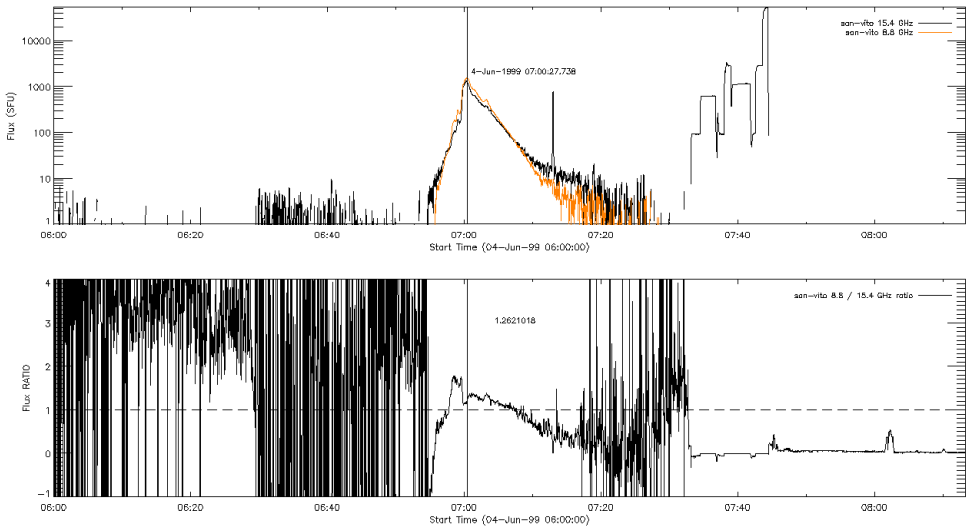

Figure 6: Example of a single peak event. For these events the selection of the time where the flux ratio is calculated is unique.

events can be seen in Figure 7. A direct comparison with a signature of gyro-synchrotron emission of a single peak event shown in Figure 6, illustrates that the thermal events have a low flux density (typically well below 100 sfu) and a slower evolution than the gyro-synchrotron bursts. These events return an erroneous prediction as this flux ratio is not describing a physical quantity related with the accelerated protons observed in-situ.

3.5 Confined Events

Chertok et al (2009) describes the relationship between the characteristics of the microwave spectrum resulting from accelerated particles at the flare site and the SEP spectrum observed in-situ. A physical relationship between the microwave spectrum at the Sun and the proton spectrum near 1 AU can only exist if the microwave-emitting electrons and the presumably associated protons escape into space to be detected. If a specific event is confined, which means that the magnetic topology does not allow a direct escape of the accelerated particles, the microwave $S_{8.8}/S_{15.4}$ ratio cannot predict the characteristics of the SEP spectrum. This is the case of event 18 observed on 2005 July 14. A way to asses the direct escape of particles from the flaring site is to verify the presence of type III radio bursts at deca-hectometric (DH) frequencies. DH-type III bursts are clear signatures of escaping electron beams. In Figure 8 is shown an overview plot of the event. We can notice the lack of a clear DH-type III at the time of the 15.4 GHz emission peak.

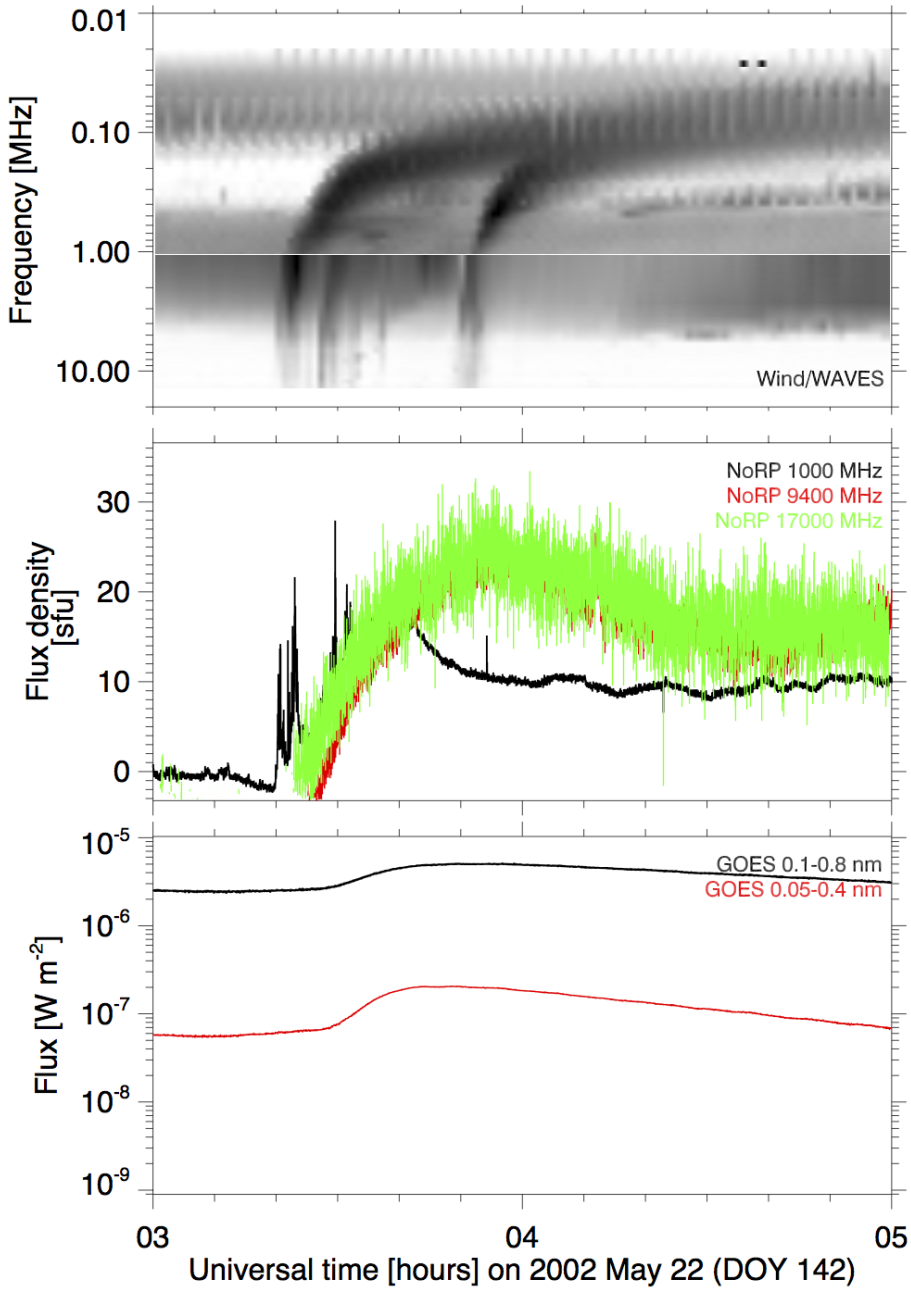

Figure 7: Example of a thermal event. This events have usually a low flux density of microwave emission and the show a slow decay in time. The ratio of the $S_{8.8}/S_{15.4}$ is $\sim$1 in these cases.

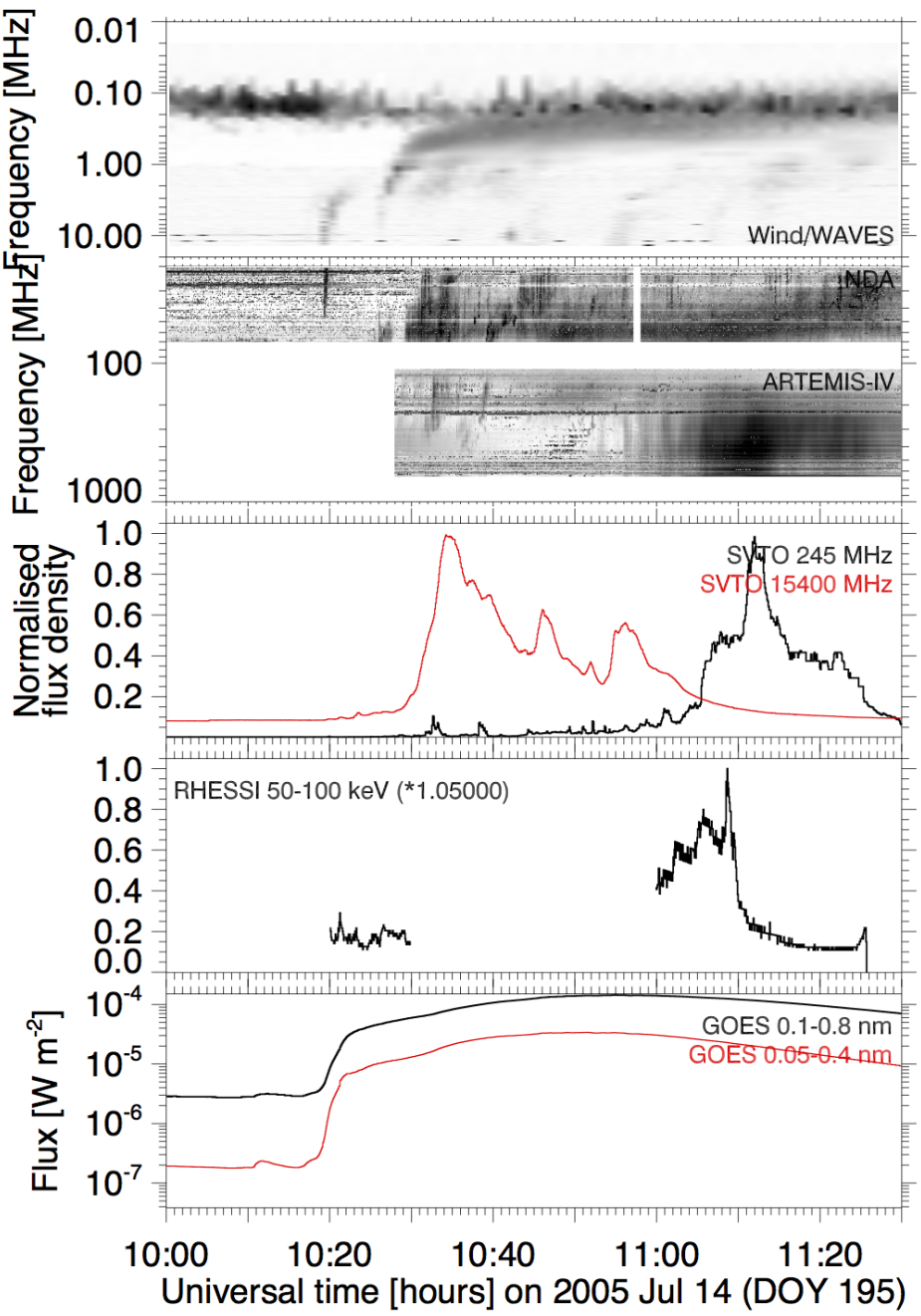

Figure 8: Example of a confined event. This event do not show a clear signature of type III burst at the time of the microwave emission.

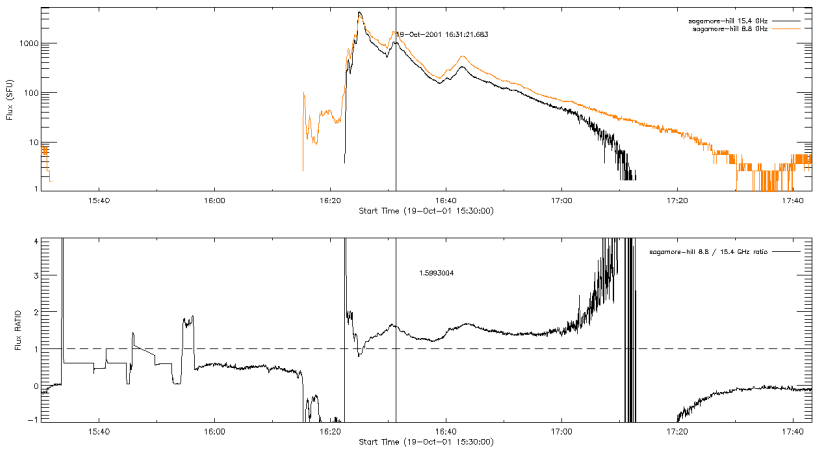

Figure 9: Example of a multiple peak event where the ratio may change between different peaks to return different prediction.

3.6 Wrong peak selection

In the presence of multiple microwave peaks a discriminative criterium to identify the correct time to calculate the $S_{8.8}/S_{15.4}$ ratio may be the verification of the presence of a DH-type III burst. One example event can be identified on 2001 October 19. This example shows how the ratio of the microwave flux density may change during the same event at different peaks, returning different predictions depending on the selected peak. In Figure 9 the flux density of a multi peak event is shown. We can note that the first peak returns a hard spectral prediction while the second and third peak return a soft spectrum as measured in the related SEP event. In this case we can verify that the first peak does not show a clear signature of escaping particles and therefore it's a confined event. This is evident in Figure 10 where we can see that no type III radio burst was observed at the time of the first peak. It is not surprising that a confined event returns an erroneous prediction. In this case even if this peak presents the strongest emission, it is discarded as it is confined and the correct prediction is obtained from the second peak.

Some events however, may show multiple flares with the associated DH-type III. On 2000 November 24 three different flares resulting in three sets of multiple microwave emission peaks were observed. Figure 11 shows the microwave $S_{8.8}$ and $S_{15.4}$ intensity and ratio. The timing of the microwave emission and the radio DH-type III bursts can be compared in Figure 12. All thee microwave bursts are accompanied by DH-type III bursts. Even if they are weaker at the time of the first two flares, and a strong and clear type III is recorded for the third flare we cannot exclude a priori that the first two flares are responsible for the accelerated particles. In addition, as shown in Figure 11 the value of the $S_{8.8}/S_{15.4}$ ratio and the associated prediction changed not only between different flares, but also at different peaks of the same flare (as for the third flare), so the situation is more complicated. If

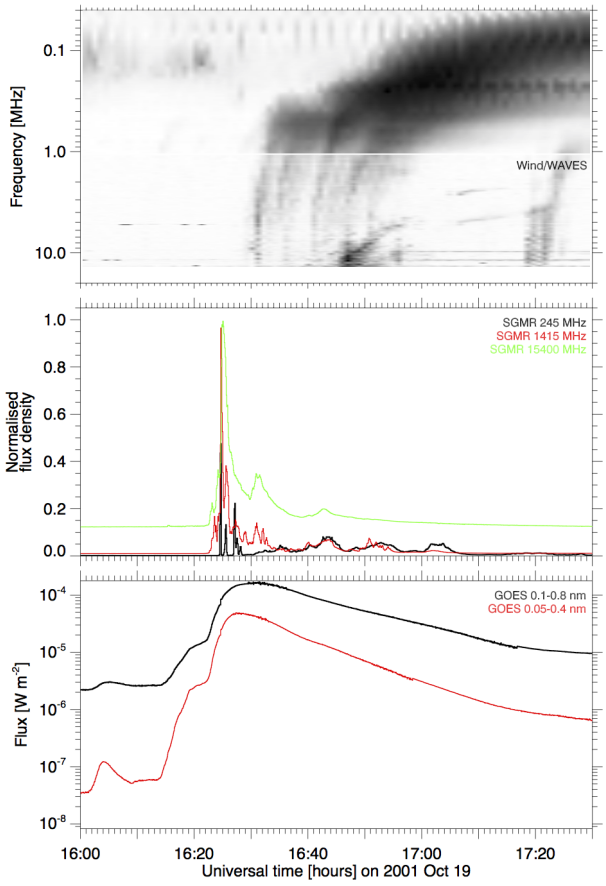

Figure 10: Multiple peak event.

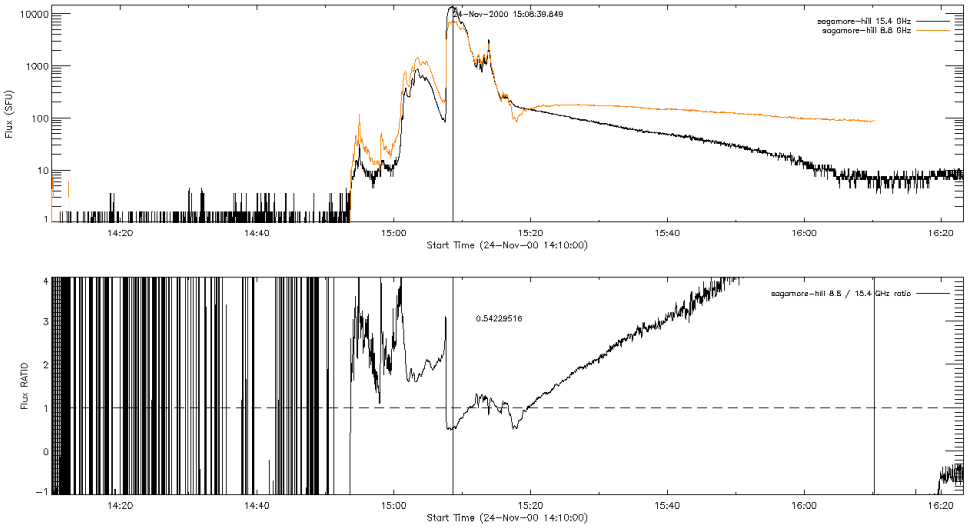

Figure 11: Example of a multiple peak event.

we consider the totality of the event (i.e. the three flares), the first two flares show a soft ratio, while the third flare shows one peak with hard ratio and one with soft ratio, with a overall dominance of a soft ratio. A method to consider for such complicated events with the presence of multiple ratio predictions, could be the evaluation of the most frequent ratio for the entire event, as the most frequent ratio might be more plausibly representative of the characteristics of the accelerated particles observed in-situ. An uncertainty on the peak selection is nevertheless to be taken into account when applying the microwave ratio prediction for these complicated events.

3.7 Instrumental problems and corrupted data

Another issue that might arise when evaluating the $S_{8.8}/S_{15.4}$ ratio is a data-quality or instrumental problem. We show here an example of microwave light-curves where the receivers are saturated and therefore returning a wrong ratio value. Figure 13 shows an example of such events. The event on 2003 October 28 shows a clear flat peak resulting from instrumental problems probably due to saturation of the receivers. This event should to be excluded from the sample.

3.8 Occulted / Partially occulted events

When the active region where the flare is produced is close to the limb or in certain cases occulted or partially occulted by the solar disk, the weak microwave emission observed can not be used to measure a precise $S_{8.8}/S_{15.4}$ ratio. These events are normally excluded from the study, such as the event on 1998-Nov-14, which did not show any microwave emission.

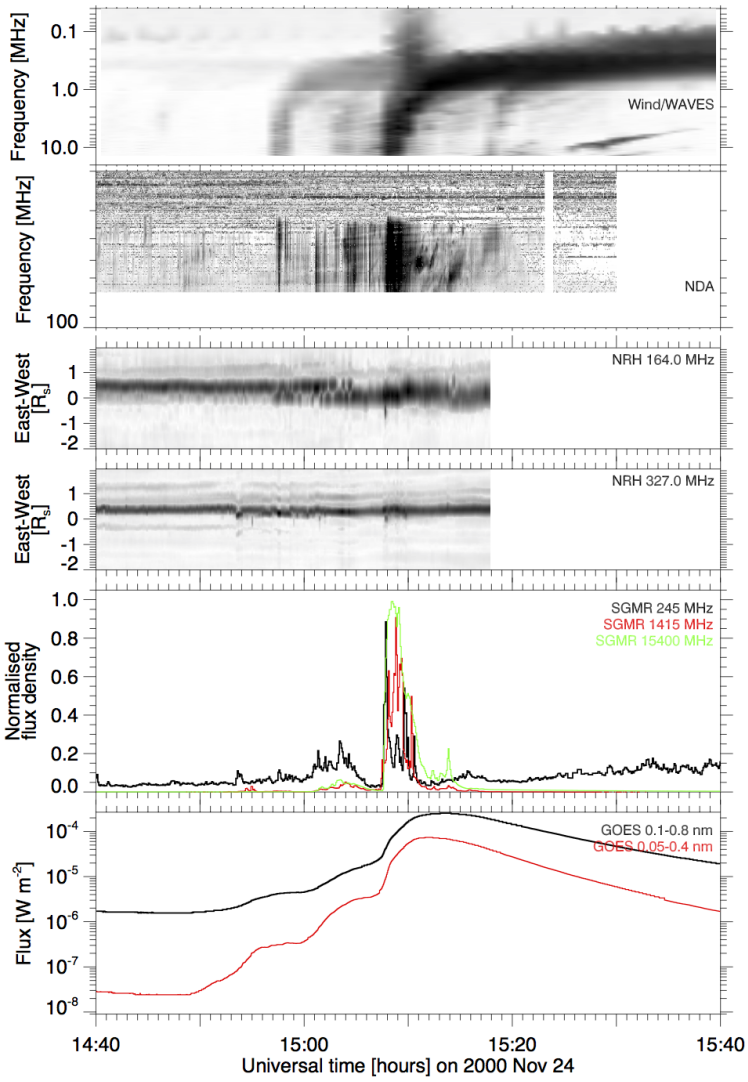

Figure 12: Microwave flux and radio spectrum observed on 2000 November 24.

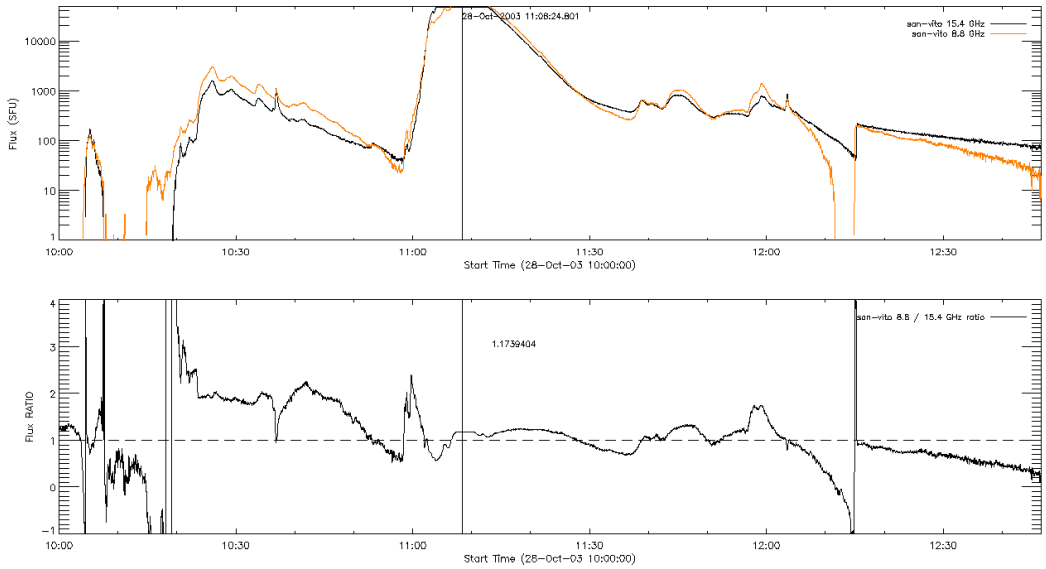

Figure 13: Example of a saturated peak flux density returning an erroneous ratio. The event was observed on 2003 October 28.

However for this preliminary study we included events close to the limb showing a weak microwave emission to test their behaviour in predicting the SEP spectra. On 2005 June 16 an event occurring close to the west limb was partially occulted and the microwave flux density was weak (<100 sfu) due to the partial occultation. The calculated ratio returned an erroneous prediction, as the observed flux is partially occulted and therefore not indicative of the real emission. These partial occulted events need to be excluded from the study as well as the fully occulted events.

3.9 Failures of the Chertok prediction scheme

In the sample of 47 events and in the subset of the 8 failed prediction we identify one event for which the criteria simply fails without a clear reason such as the ones explained in the previous sections. The microwave flux and the ratio for the event observed on 1998 May 02 are shown in Figure 15. We can notice in this case the presence of multiple microwave peaks, all returning a value of the $S_{8.8}/S_{15.4}$ ratio higher than 1 and therefore predicting a soft particle spectrum. This particular event was not occulted, nor did it present anomalies in the data-quality. This prediction error is therefore to ascribe to the limitation of the method. The related SEP time profile is shown in Figure 16.

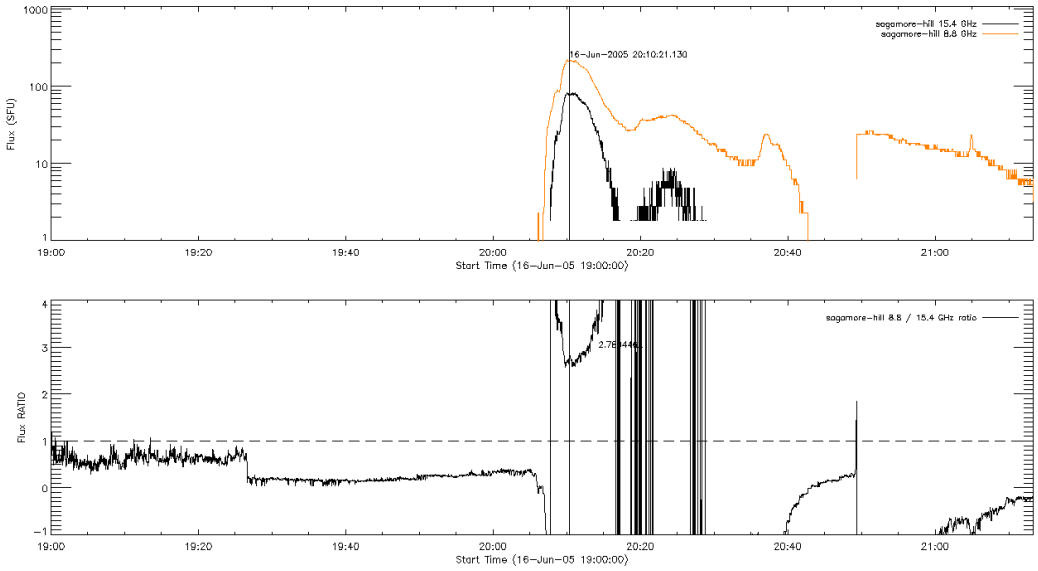

Figure 14: Example of a weak flux density from an occulted limb event returning an erroneous ratio. The event was observed on 2005 June 16.

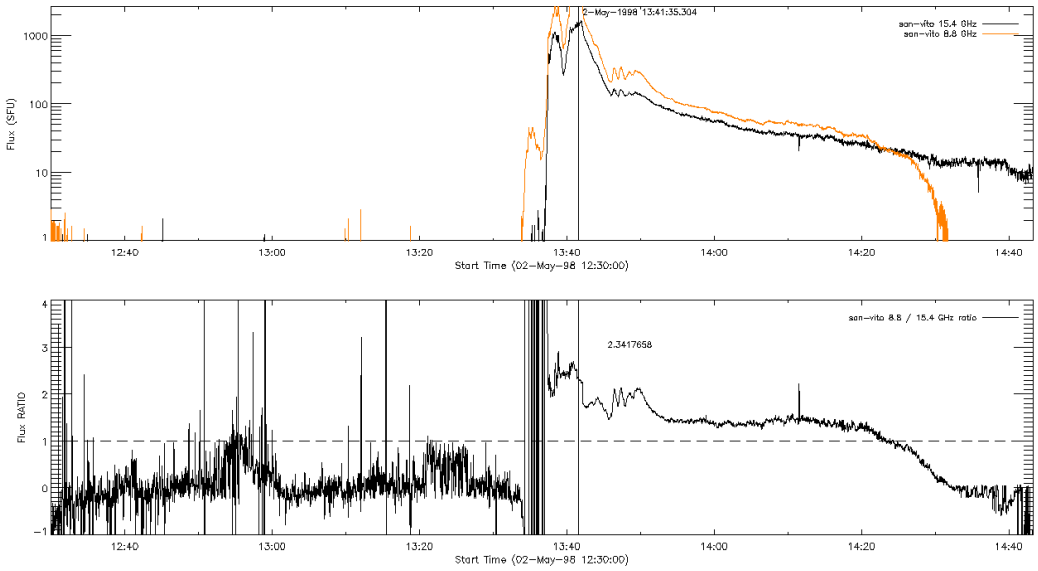

Figure 15: Example of an event where the Chertok relation do not predict the SEP spectra correctly. The event was observed on 1998 May 02.

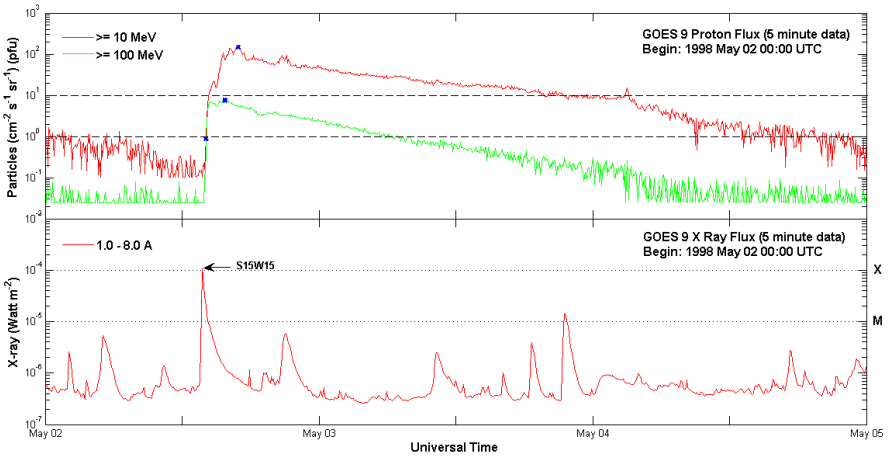

Figure 16: SEP time profile of the event observed on 1998 May 02 and returning a wrong prediction.

3.10 Peak frequency and sampling limitations

As introduced in Section 2, the microwave spectrum is optically thick below the peak frequency, and optically thin above. The spectral index in the optically thin part is directly related to the index of the energy spectrum of the radiating electrons. A criterium to assess if we are in the optically thick part of the gyro-synchrotron spectra is therefore the evaluation of the peak frequency. The value of the peak frequency is reported for all the events on Table 1, we can notice that all the events with hard prediction show a peak frequency of 15.4 GHz or more. The maximum frequency observable by the RSTN network is 15.4 GHz and this may result in a limitation. For some of the events such as events 16 and 23 and where data is available we used Nobeyama (maximum observing frequency 35 GHz) to verify if the peak frequency was higher than 15.4.

4 Analysis of all events

We compared this sample of 47 events with what was found by Chertok et al (2009), the scatter plot showing the correlation between δ and $S_{8.8}/S_{15.4}$ is shown in Figure 17. For our sample or 47 events we found a linear correlation of $\delta = 0.5(S_{8.8}/S_{15.4}) + 1.2$ similar to Chertok's results $\delta = 0.6(S_{8.8}/S_{15.4}) + 1$. We were able to predict the SEP spectral hardness correctly for 39 events, with 8 events ($\sim$20%) returning a false prediction. The events with a false prediction are indicated in Figure 17 by red squares, while the events with hard prediction are indicated by blues dots, and the events with soft prediction are indicated with red dots.

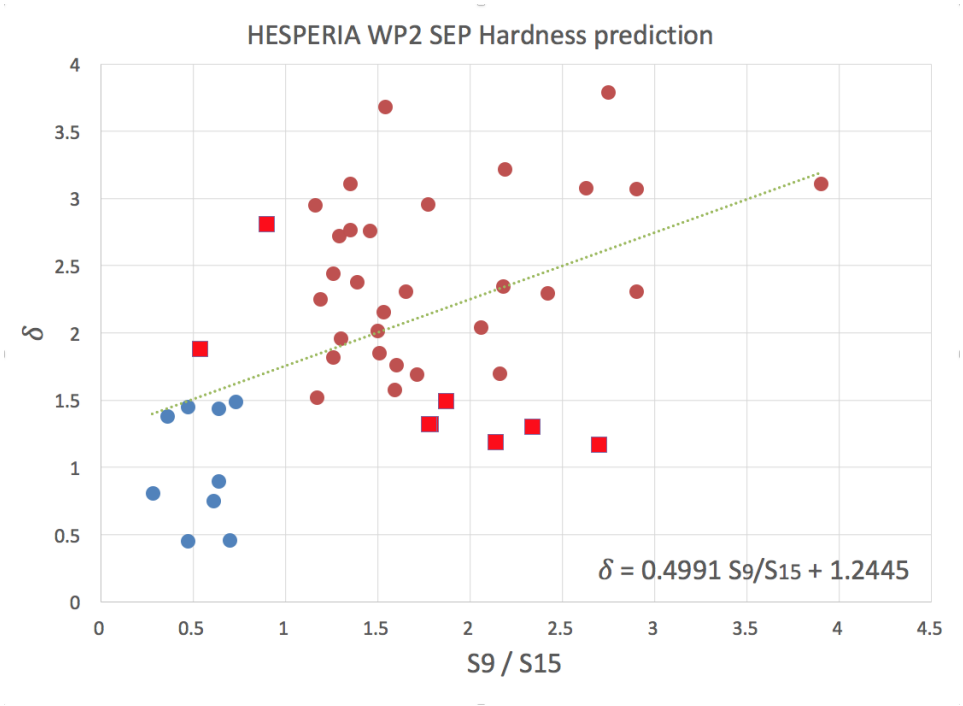

Figure 17: Scatter plot of the 47 events. With the blue circles are marked the hard spectral prediction, with the red circles the soft predictions, while the erroneous predictions are marked with red squares.

4.1 Multi-Peak analysis

We repeated the analysis of the microwave flux density ratio for each event with a multiple emission peak. An example plot showing the ratio calculated for the different peaks is shown in Figure 18. The ratio $S_{8.8}/S_{15.4}$ was extracted for all peaks for each event, this extended analysis is reported in Figure 19. This extended analysis was performed to investigate the sources of the scattering of the data-points depending on the different values of microwave flux density ratio for each peak. Single peak events are reported in orange, while multi peak events are in blue. Confined events are marked with yellow squares, while thermal events are reported in triangles.

5 Statistical evaluation: probability of detection and false alarm rate

Microwave data might be available in real-time in the future and then serve as a real-time prediction of the SEPs energy used in conjunction with the UMASEP prediction. For

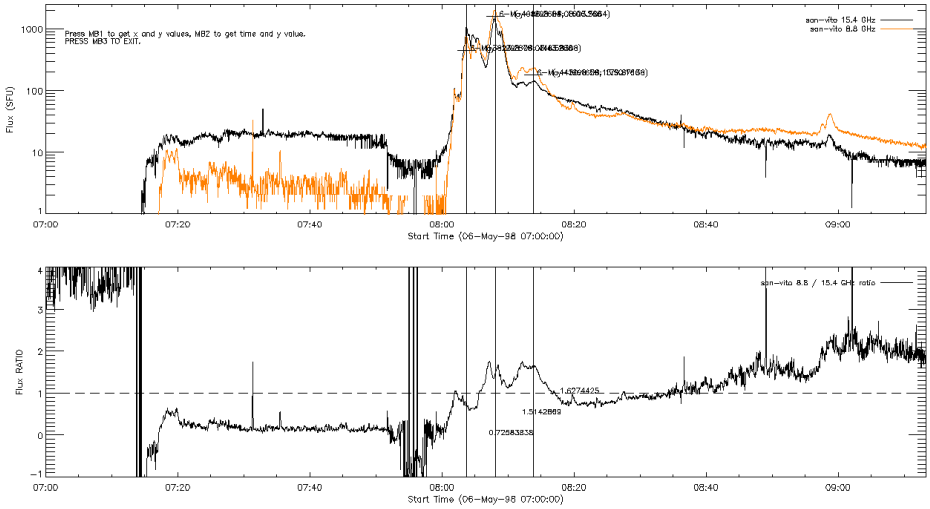

Figure 18: Example event where the ratio was calculated at each peak.

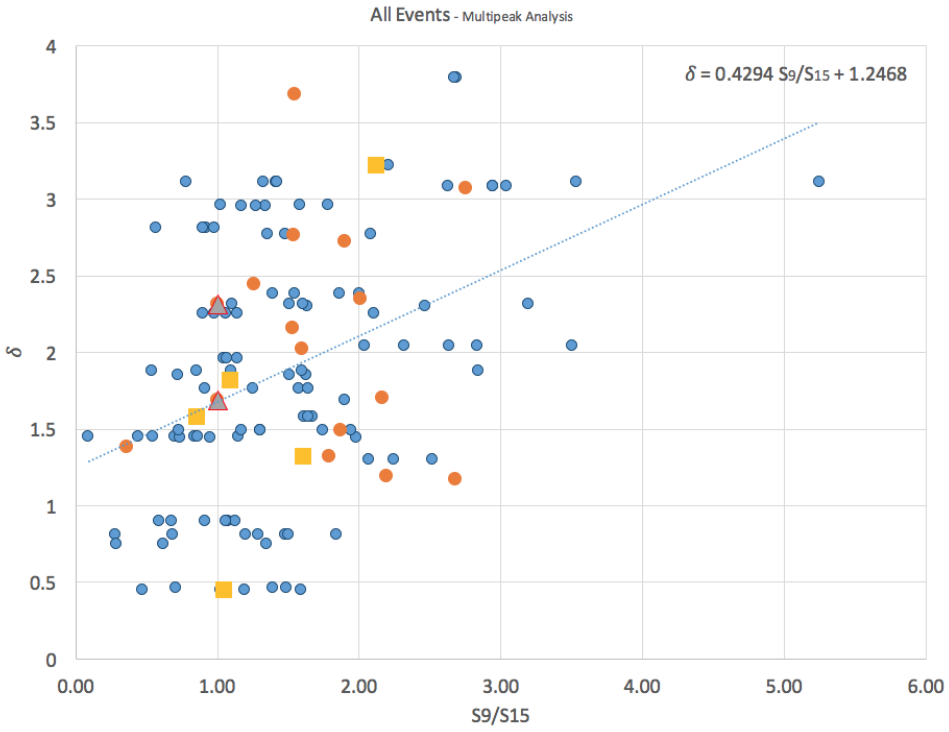

Figure 19: Scatter plot including the ratio calculated for the multi-peak events. Single peak events are reported in orange, while multi peak events are in blue. Confined events are marked with yellow squares, while thermal events are reported in triangles.

this reason, it is important to estimate the prediction performance of techniques for predicting hard/soft SEP spectrum from microwave emissions from the operational point of view by calculating the probability of detection (POD) and the false alarm ratio (FAR). In order to assess the performance of the prediction of the proton spectral hardness using microwave emission, we calculate the corresponding POD_H and FAR_H. To assess the performance of the proton spectra softness prediction, we calculate the corresponding POD_S and FAR_S. We decide to select the S9/S15 threshold such that soft proton spectra are predicted when S9/S15$>$ 1, and hard proton spectra when S9/S15 $<$ 1. In order to estimate POD_H and FAR_H, we need to calculate the following variables: AH, which is the number of correct predictions (i.e. hard spectrum predicted, and hard spectrum observed); BH, which is the number of erroneous predictions (i.e. hard spectrum predicted, but soft spectrum observed); and CH, which is the number of missed events (i.e. soft spectrum predicted, but hard spectrum observed). By using these variables, the POD_H is calculated as AH/(AH+CH), and FAR_H is calculated as BH/(BH+AH). The column 2 in Table 2 presents the quality of the prediction for each event, where a, b and c indicate a successful prediction, an erroneous prediction and a missed event, respectively. According to column 2 of Table 2, we obtain the following results: AH, the number of successful hard spectrum predictions is 9; BH, the number of erroneous hard spectrum predictions is 2; and, CH, the number of missed hard spectrum SEP events (listed in Table 1) is 6. By using these counters, the POD_H is 60% and the FAR_H is 18.2%. In order to estimate the performance of soft spectrum predictions, we estimate POD_S and FAR_S by calculating the following variables: AS, which is the number of correct predictions (i.e. soft spectrum predicted, and soft spectrum observed); BS, which is the number of erroneous predictions (i.e. soft spectrum predicted, and hard spectrum observed); and, CS, which is the number of missed events (i.e. hard spectrum predicted, and soft spectrum observed in Table 1). According to column 3 of Table 2 we obtain the following results: AS is 30; BS is 6; and, CH is 2. By using these counters, POD_S is 93.8% and the FAR_S is 16.7%, which is a very satisfactory performance. One of the purposes of Task 2-2 is to study the possibility of finding empirical rules or conditions that yield better SEP spectrum prediction performance. With this purpose, we found that all successful hard spectrum predictions were associated with M6 flares, and that one of the erroneous predictions was associated with a lower intensity class flare; this finding suggests us that if the Chertok et al's technique is triggered only when the associated flare is M6, the forecasting performance metrics, say $\mathrm{POD}_{H'}$ and $\mathrm{FAR}_{H'}$, are slightly better. By using this empirical triggering condition, the quality of the predictions (indicated in the column 4 of Table 2) may summarised as follows: AH' is 9; BH' is 1; and, CH', the number of events (associated with M6 flares in Table 1) is 4. With these counters, the $\mathrm{POD}_{H'}$ is 69.2% and the $\mathrm{FAR}_{H'}$ is 10%.

	Hard spectrum predictions[1]	Soft spectrum predictions[2]	Hard spectrum predictions (with triggering conditions)[3]
1	a		a
2	c	b	c
3		a	
4		a	
5		a	
6	b	c	d
7		a	
8		a	
9	c	b	d
10	a		a
11		a	
12	a		a
13		a	
14	a		a
15		a	
16		a	
17		a	
18	a		a
19	c	b	c
20		a	
21	c	b	c
22		a	
23		a	
24		a	
25		a	
26		a	
27		a	
28	c	b	
29		a	
30		a	
31	a		a
32		a	
33		a	
34		a	
35		a	
36		a	
37		a	
38		a	
39	a		a
40	c	b	
41	b	c	
42		a	
43		a	
44	a		a
45		a	
46	a		a
47		a	

[1] Hard SEP spectrum predictions from hard spectrum of microwave emissions according to the technique proposed by Chertok et al (2009).
[2] Soft SEP spectrum predictions from soft spectrum of microwave emissions.
[3] Hard SEP spectrum predictions from hard spectrum of microwave emissions according to the technique proposed by Chertok et al (2009) applied only to those observed events associated with M6 flares.

Table 2: Quality of hard and soft SEP spectrum predictions.

6 Summary

We analysed 47 events using remote-sensing microwave observations and we were able to correctly predict the spectral characteristics of SEPs observed in-situ for 39 events with 8 events ($\sim$20%) returning a false prediction. We analysed the reasons for the false predictions in order to improve the method and study the use of extra proxies for the prediction such as the peak frequency. We found sources of spurious calculation of the ratio due to the presence of multiple peaks in the microwave flux density. We show how a particular attention in the selection of these peaks verifying the presence of escaping particles (presence of type III radio burst) may improve the prediction method. We identified also the presence of emission due to thermal particles, which could not be used as proxy for the SEP spectral characteristics.

References

Chertok IM, Grechnev VV, Meshalkina NS (2009) On the correlation between spectra of solar microwave bursts and proton fluxes near the Earth. Astronomy Reports 53:1059–1069, DOI 10.1134/S1063772909110110